## 1.5 INVASIVE CARCINOMAS

The hallmark of invasive carcinomas is migration of the cancer cells through the dissolved basement membrane into the stroma. The tumor cells leave the well-defined structures (ducts and lobules) of the lobe (Fig. 1.35).

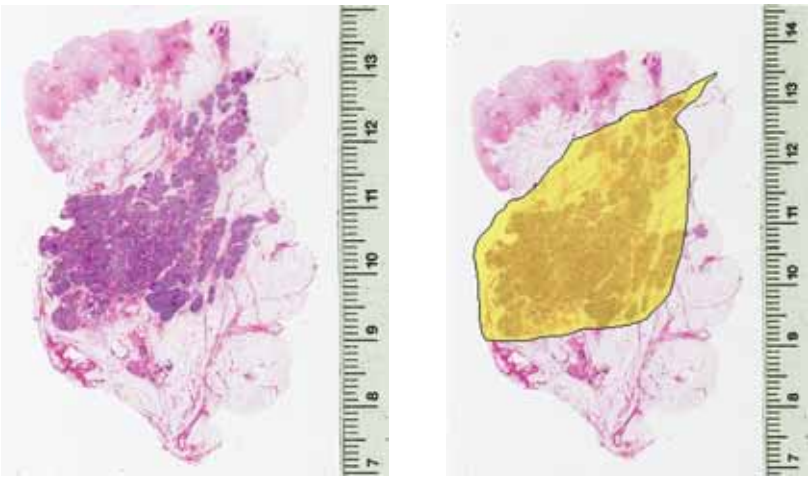

(a) (b)

**Figure 1.34** Involvement of the duct system in cases of ductal carcinoma in situ leads to the development of diffuse lesions, which are not well circumscribed and are difficult to outline and measure. (a) Large histological section, and (b) extent of the disease.

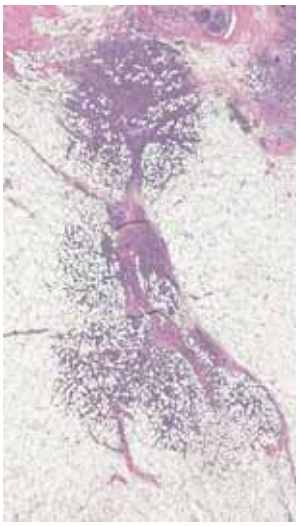

**Figure 1.35** The hallmark of invasive carcinomas is migration of tumor cells from the ducts and lobules through the dissolved basement membrane into the stroma.

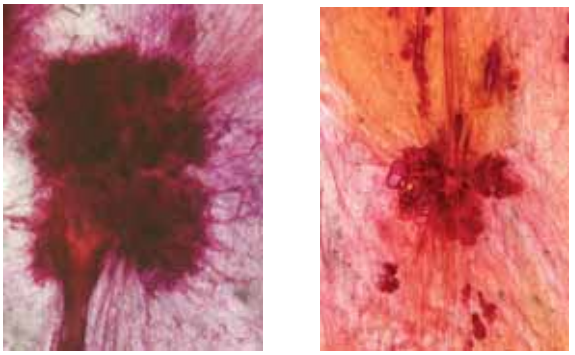

(a) (b)

**Figure 1.36** Thick section images of (a) invasive carcinoma, and (b) radial scar.

(a)

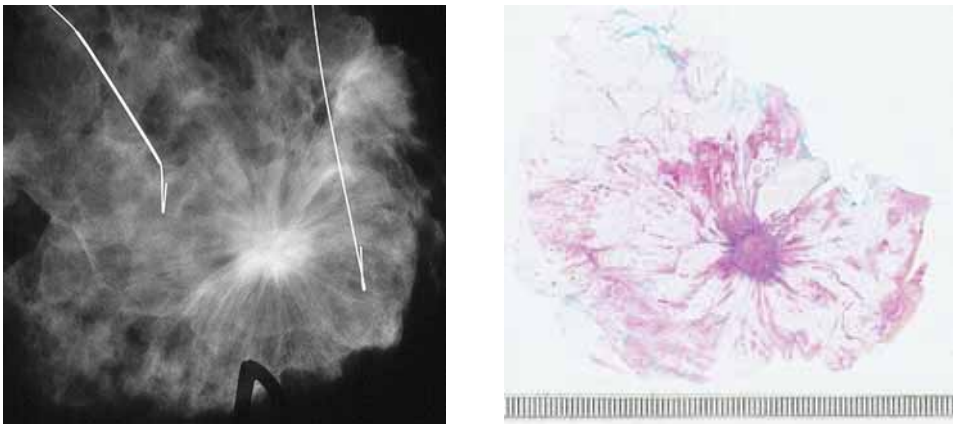

(b) (c)

**Figure 1.37** Spiculated tumor mass is the most usual manifestation of invasive carcinomas. (a) Macroscopic image, (b) radiologic image, and (c) histologic image.

Invasion most often evokes proliferation of fibroblasts and myofibroblasts as well as collagenization in the stroma damaged by the tumor cells—a reaction called stromal desmoplasia, which prevents the tumor cells from invading the stroma evenly in all directions. This process leads to the development of a spiculated ("stellate") tumor mass, the most usual manifestation of invasive carcinoma. Figure 1.36(a), demonstrates a 3D image of such a tumor and compares it to the 3D image of a radial scar [Fig. 1.36(b)]. The typical macroscopic appearance of a stellate carcinoma is illustrated in Fig 1.37.

About two-thirds of invasive carcinomas are of stellate shape. The shape of the invasive tumor is related to its histologic type. The stellate carcinomas are most often invasive lobular, tubular, or grade I or grade II invasive ductal not otherwise specified (NOS) cancers (see Diagram 1.5); these together correspond to more than 80% of stellate tumors.

Benign stellate lesions are rare. Only the appearance of elastic fibers in the stroma (as in radial scars) or collagenization due to scar formation leads to lesions imitating the stellate shape of breast carcinoma. Thus, a stellate lesion on a mammogram is most often (in more than 90% of cases) malignant and warrants further diagnostic and therapeutic interventions.[1,9] Although spiculated, radial scars lack a well-formed tumor body [Fig. 1.38(a)] and appear as "black stars" on a mammogram [Fig. 1.38(b)]—in contrast to the "white stars" in carcinoma cases [Fig. 1.37(b)]. The histologic appearance is also typical as they exhibit an elastic core and a corona of hyperplastic changes [Fig. 1.38(c)]. In a minority of cases, radial scars may contain low-grade in situ carcinoma foci in their corona and represent a "special type" of in situ cancer.

If the desmoplastic stromal reaction on invasion of the tumor cells is weak or absent, the cells may invade evenly in all directions, giving rise to a circular (or oval) tumor mass. These tumor masses are similar to benign or malignant lesions

**Diagram 1.5** Distribution of 910 consecutive stellate invasive carcinomas by tumor type, Falun 1996–2003.

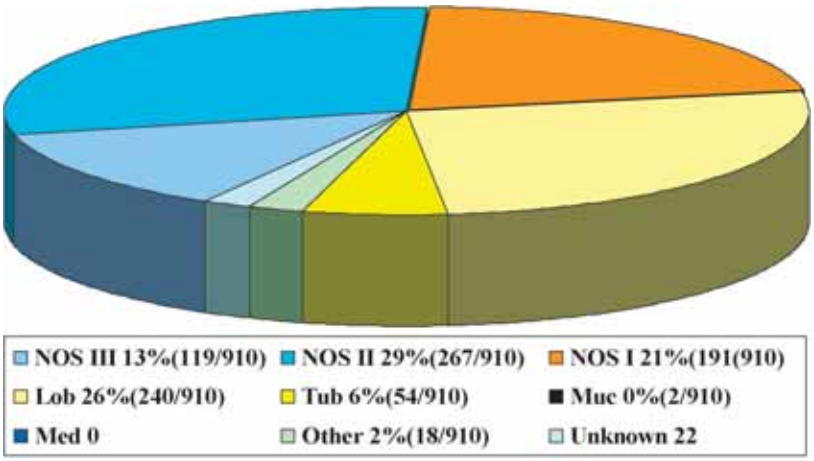

## 9.1 DETECTION OF MICROCALCIFICATIONS: BACKGROUND AND MOTIVATION

In Western countries, women have a higher than 1-in-8 chance of developing breast cancer during their lives. Breast cancer represents the most frequently diagnosed cancer in women.[1] The National Cancer Institute of U.S.A. estimates that, based on current rates, 13.2% of women born today will be diagnosed with breast cancer at some time in their lives.[2]

In order to reduce mortality, early detection of breast cancer is important, because therapeutic actions are more likely to be successful in the early stages of the disease. For women whose tumors were discovered early by mammography, the five-year survival rate was about 82% as opposed to 60% for the cases where the tumors were not found early.[3]

Mammography is currently the best radiological technique available for early detection of nonpalpable breast cancer. However, it is difficult for radiologists to provide both accurate and uniform evaluations for the large number of mammograms that they have to interpret in screening programs where most of the cases are normal; it has been observed that 10–30% of breast lesions are missed during routine screening.[4] The situation is even more challenging since the early malignancies have small size and subtle contrast when compared with normal breast structures. Double reading (as carried out, for example, by two radiologists) helps to reduce the number of false negatives by 5–15%.[5,6]

Digital image-processing techniques represent useful tools for helping radiologists to improve their diagnosis with the aid of computer systems. In this sense, different CAD (computer-aided diagnosis) tools have been developed for improving image quality, identifying malignant signs, enhancing mammographic features, etc. On the average, the reader's sensitivity can be increased by 10% with the assistance of CAD systems.[7] Some works have studied this potential of CAD to improve radiologists' performance in detecting clustered microcalcifications.[8]

There are a number of different classes of abnormality that may be observed in mammograms. One of the most significant types of mammographic abnormality is microcalcification. Microcalcifications are tiny granule like deposits of calcium. They are relatively bright (dense) in comparison with the surrounding normal tissue,[9] and are up to about 1 mm in diameter, with an average diameter of 0.3 mm. Microcalcifications are of particular clinical significance when found in clusters of three or more within a square-centimeter region of a mammogram.[10] Lanyi[11] has described microcalcifications as "the most important leading symptom in mammographic detection of preclinical carcinomas." Sickles[12] noted that more than 50% of nonpalpable cancers had mammographically visible calcifications, and in 36% of nonpalpable cancers, calcifications were the only sign of abnormality. In an important study of cancers missed in screening mammography, it was observed that the presence of microcalcifications was the predominant feature in 18% of the missed cancers.[13]

Although computer-aided mammography has been studied for more than two decades, automated interpretation of microcalcifications remains a challenge due to their small size and variable appearance. Furthermore, when located within or superimposed by dense tissues, especially in young women, microcalcifications have almost the same brightness level as the background tissue, which makes them difficult to detect. In view of the above, it is evident that methods for automatic detection of microcalcifications in mammograms are desired in order to assist radiologists in the interpretation of mammograms and the diagnosis of breast cancer.

## 9.2 STATE OF THE ART

### 9.2.1 MICROCALCIFICATION DETECTION

The problem of detection of microcalcifications in digitized or digital mammograms has been addressed for almost three decades. During this period the sensitivity of detection has been improved, with some recent papers reporting more than 90% sensitivity. Nevertheless, the false-positive rate remains high, especially when detecting individual microcalcifications.[4] Initial studies on the detection of microcalcifications date from the 1970s and were based on hard-decision rules applied to features that described a given mammogram locally, such as local maxima, contrast, and compactness.[14] Recent methods are designed to extract features from a more detailed analysis of the mammogram, and detect microcalcifications by applying the features to classification tools such as neural networks or support vector machines (SVM). Due to the difficulty in detecting microcalcifications, especially in dense mammograms, where the background has an intensity similar to that of the microcalcifications, an enhancement step is usually added to the CAD tool to detect microcalcifications. The general scheme of a microcalcification-detection CAD tool is summarized in Fig. 9.1. Recent research on this topic has been focused on improving one or more of the blocks that appears in Fig. 9.1.

#### 9.2.1.1 Enhancement

In the first step, a general technique to increase the contrast can be applied. In this way, Nam and Choi[15] applied histogram equalization and contrast enhancement to the problem of detecting microcalcifications. In the same way, many techniques

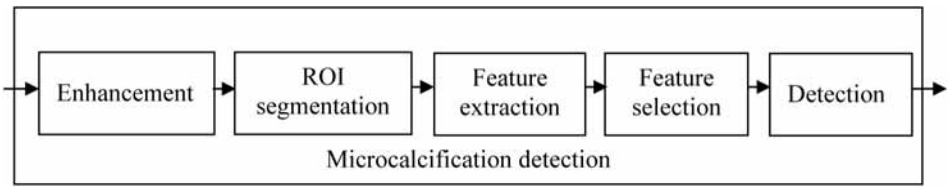


**Figure 9.1** General scheme of the microcalcification-detection part of a CAD tool.

## 11.1 INTRODUCTION

Accurate skin-line estimation is an important prerequisite for enhancement and analysis of mammograms for computer-aided diagnosis (CAD) of breast cancer. Appropriate display of benign and malignant lesions inside the breast region in mammograms has a direct relationship to the skin line of the breast. Even a small window/level operation on a digital display by a radiologist to enhance the visibility of lesions inside the breast region can lead to diminished skin-line information due to the loss of gray-level contrast. In this process, a lesion located near the skin-line may also be lost. This is attributed to the fact that the breast tissue in the skin-line zone is less dense compared to the other tissues in its neighborhood (see Fig. 11.1). Although the above fact poses an inherent challenge, there are other challenges such as noise present in low-contrast mammograms.[1] The noise can come from digital-or film-acquisition processes called "system noise." Besides the structural and systemic challenges, automatic skin-line estimation is hindered by extraneous structures in x-ray mammograms such as labels for patient identification, especially when the labels are placed close to the breast. It is proposed to solve such difficult cases by our novel automatic skin-line detection strategy. The variability present between the images in a data set due to breast size and proto-

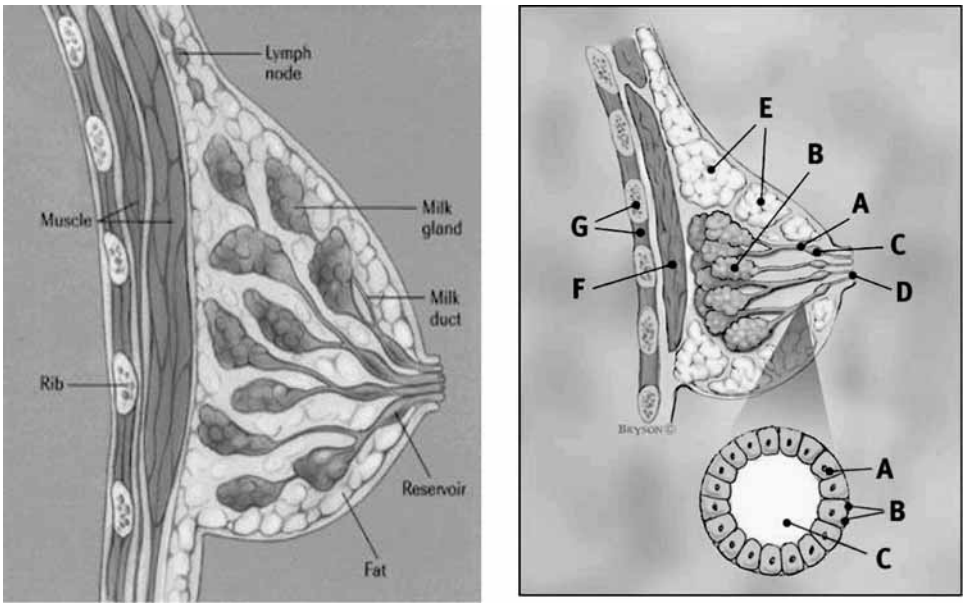


**Figure 11.1** Illustration of the anatomy of the breast. For labels in the breast of the right side image: (a) ducts, (b) lobules, (c) section of duct to hold milk, (d) mammilla, (e) fat, (f) pectoralis major muscle, (g) chest wall/rib cage. For labels in the lower magnified view: (a) normal duct cell, (b) basement membrane, (c) lumen (center of duct). (Reprinted with permission from Ref. 11, Copyright Health Communities. Com, Inc.) Refer to the CD for the full color figure.

cols of image acquisition can make a skin-line detection system complex. Having discussed the prominent challenges posed in automatic breast skin-line estimation, previous related works by other research groups are reviewed.[2–7]

After carefully evaluating the strategies used by other research groups for skin-line estimation, the proposed algorithms are classified into primarily two categories: (1) histogram-based thresholding, and (2) the boundary-based deformable model. The technique is novel: a combination of knowledge regarding the anatomy of the breast, and constraints between the skin-line boundary and the edge of the stroma of the breast are introduced. In essence, the algorithm is a hybrid approach with several novelties.

Algorithms in the thresholding-based category have been used to get separate masks for the different breast regions.[3–5] Because of different densities in the breast region, thresholding-based strategies are susceptible to erroneous thresholds, which could result in multiple objects/regions, and demands extensive local processing such as region growing and morphological filtering. Abdel-Mottaleb et al.[4] proposed a multiple thresholding method to estimate the skin line and improved the statistics of acceptability.

In the category of thresholding, a significant advancement was achieved by Ojala et al.[5] Their method was adaptive in nature, and their concept for segmentation of the breast region was based on the assumption that there is a discontinuity of histogram values between the breast region and the background. Thus, they attacked the problem of threshold detection and optimized their objective function. Their threshold-based method is a rationalized approach, and independent of breast density, size, and view. This approach was chosen as a part of one of the strategies to take advantage of its merits.

A different approach is the boundary-based deformable model, in which parametric snakes have been applied.[1,6,7] Wirth and Stapinski[6] used a combination of Rosin's thresholding method[8] and the greedy active-contour method. The method was applied to a small selection of 25 mammograms from the MIAS database.[9] In the same class of algorithms, Ferrari et al.[2] improved the snake model to make it adaptive. The adaptive active deformable model improved an initial contour obtained using a threshold derived by the Lloyd-Max quantizer.[10] A combination of the quantizer with the adaptive greedy approach reduced the mean skin-line estimation error when compared to ground-truth skin lines traced by an expert radiologist. Although our approach is not purely elastic-based, our constraints are elastic in nature, which pulls or pushes the boundaries toward the most stable state of the skin line.

A brief summary of our approach is as follows. An initial estimate of the skin line is obtained by adaptive thresholding based on the local discontinuity between the breast area and the background. It is assumed that the initial skin line will not be accurate in the upper or lower portions of the breast due to background noise and artifacts. Therefore, a greedy range-selection method is used to select a smooth and acceptable portion from the initial skin line. The greedy method yields an initial confirmed portion of the skin line around the central nipple area. Our dependency

approach consists of using the anatomic knowledge of the stroma to develop a constraint between the confirmed portion of the skin line and the stroma edge. This step uses the density concept to develop the threshold. The stroma edge is smoothed by fitting a spline, and constraints are established between the initial confirmed portion of the skin line and the smoothed stroma edge. The constraints are then propagated toward the upper and lower breast zones to correct the weak areas of the boundary, thereby getting closer to the true edge. The propagation is performed by using a greedy approach in combination with anatomical constraints. Comparing the results of the algorithm with those of one of the best methods reported, namely the deformable model of Ferrari et al.,[2] an improvement in skin-line estimation is demonstrated by this approach. Note that the ground-truth (GT) boundaries used for the comparison were prepared and traced by radiologists.

The chapter is organized as follows. Section 11.2 presents the overall design of the system. Section 11.3 provides a description of adaptive thresholding to obtain an initial skin line. In Section 11.4, a shape analysis method for the extraction of the initial confirmed portion of the skin line is presented. In Section 11.5, the methods for the extraction of the edge of the stroma and spline fitting are presented. Section 11.6 presents the proposed dependency approach to obtain the final breast skin line. Several techniques and metrics for performance evaluation and comparison have been implemented as described in Section 11.7, including the polyline distance measure (PDM) and the Hausdorff distance measure (HDM). The results of the analysis are shown in Section 11.8, and the paper is concluded in Section 11.9.

## 11.2 A BRIEF OVERVIEW OF THE PROPOSED SYSTEM

The concept of the algorithm arises from the fact that the edge of the stroma of the breast has a usually uniform distance to the breast skin line (see Fig. 11.3). The stroma edge is not affected by the system noise because of the high contrast between the bright (dense) stroma region and the low-intensity (low-density) fatty peripheral region. The background region and the breast region are distinguished by a discontinuity in the histogram. This discontinuity may be estimated using an adaptive thresholding technique, such as the method proposed by Ojala et al.[5] This step is represented in Fig. 11.2 as block (A).

Because the stroma is a high-density zone, it can easily be masked out by a bimodality thresholding procedure. One such thresholding procedure has been proposed by Otsu,[12] which is widely accepted in medical image processing. The added advantage of Otsu's procedure for threshold computation is its simplicity. This step is identified in Fig. 11.2 as block (B). Therefore, an initial estimate of the outer- and inner-edge of the breast is obtained using two different thresholding processes, yielding initial estimates of the skin-line boundary and the stroma edge. This is shown by the parallel paths in Fig. 11.2.

Having extracted an initial confirmed portion of the skin line from the initial skin-line estimate and the accurate stroma edge information, a novel strategy to propagate or extrapolate the partial boundary to a full skin-line boundary based

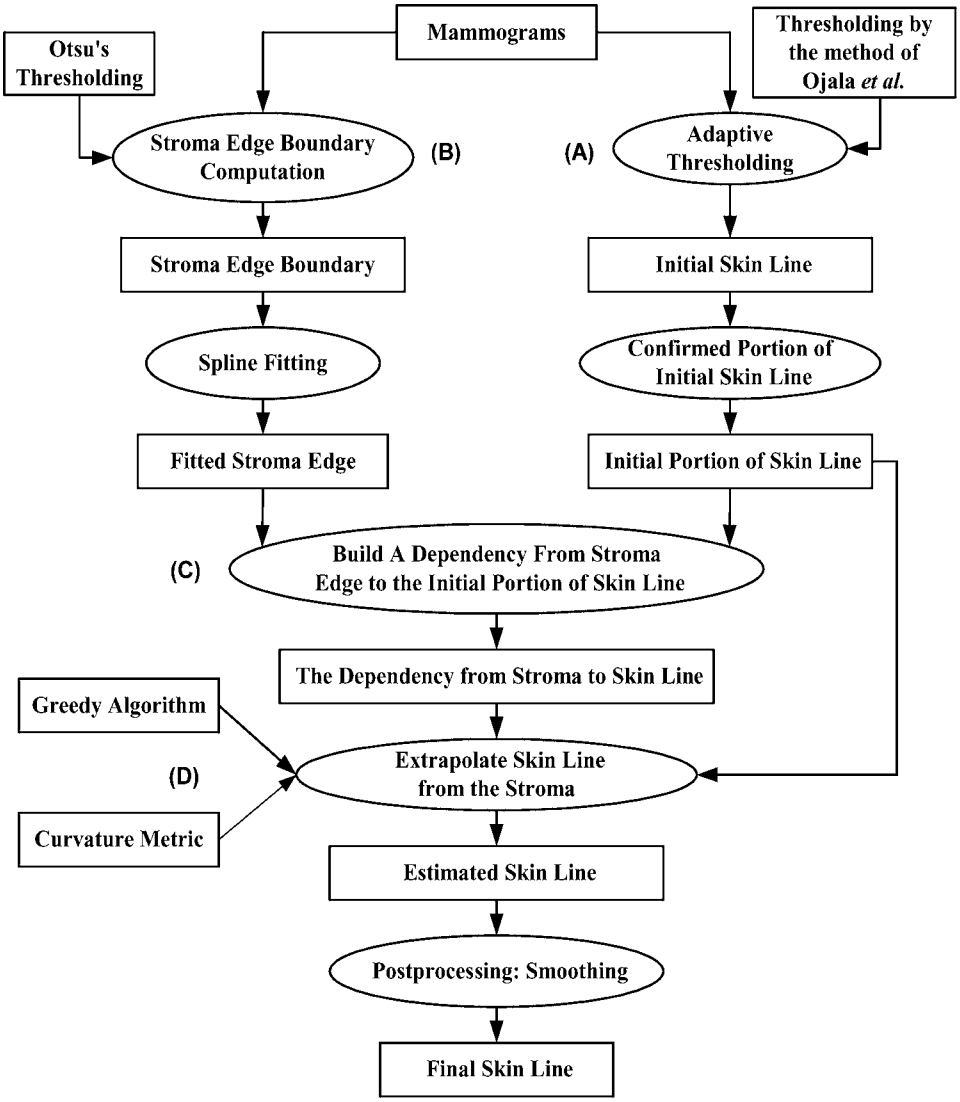


**Figure 11.2** Block diagram of the system for skin line estimation.

on constraints, called the dependency approach is proposed. This is represented by blocks (C) and (D) in Fig. 11.2. The extrapolation procedure utilizes the greedy concept and a curvature measure to yield the extrapolated skin line. The extrapolated skin line is postprocessed using a smoothing process. Ground-truth breast skin lines of the mammograms were traced by a radiologist[2] and are used to evaluate the performance of the proposed skin-line extraction system.

Figure 11.3 shows the concept of our dependency approach based on the anatomical structure of the breast. Also displayed is a mammogram showing the relative placement of the skin-line boundary and the stroma edge.

## 27.1 INTRODUCTION

### 27.1.1 ACRONYM SOUP: CAD/CADx/CAC?

*Computer-aided detection* or CAD refers to automated screening systems that localize suspicious regions in an image for a radiologist to consider (e.g., the computer marks the location of a suspicious mass or clustered calcifications using symbols on the screen). As the saying goes, "X marks the spot." These techniques can serve as a "second reader" to improve sensitivity such as to detect subtle lesions in mammography that might otherwise be missed by the radiologist. There has been a considerable body of work in this area over the past few decades.[1–13] In fact, commercial detection systems are now available that reportedly identified 77% of overlooked breast malignancies[14] and increased screening sensitivity by 20%.[15] These automated detection systems are not constrained by the limits of human vision, should be more consistent, and have the potential to improve the performance of less experienced radiologists.

Taking this one step further, predictive computer models have also been developed to characterize the status or make some recommendation for a lesion already detected by a radiologist or CAD system. Such diagnoses may go beyond a lesion to apply to a whole image, imaging study, or patient. For example, the model may predict whether a lesion is benign or malignant, or recommend a cancer patient for some therapy or not based on the likelihood of complications. This predictive modeling work is often called computer-aided diagnosis (CADx) or computer-aided classification or characterization (CAC). This is the focus of this chapter. Unfortunately, this characterization work is sometimes abbreviated to CAD, the same acronym as for detection.

To add to this confusion, most detection and characterization algorithms actually include elements of the other, such that there is no clear delineation between them anymore. For example, an algorithm to detect suspicious breast masses must not only find regions of suspicion in a mammogram, but also consider features describing each region in order to predict which ones have the highest likelihood of cancer, so as to reduce the number of false positives. Both CAD and CADx often share the same tools for image processing, machine learning, and statistical analysis. Many people simply refer to the general field encompassing both areas as computer-aided diagnosis.

### 27.1.2 CLINICAL SIGNIFICANCE

Mammography is the modality of choice for early detection of breast cancer. Although mammography is very sensitive at detecting breast cancer, its low positive-predictive value (PPV) results in biopsy of a large number of benign lesions. Of women with radiographically suspicious, nonpalpable lesions who are sent to biopsy, only 15% to 34% actually have a malignancy by histologic

diagnosis.[16,17] The excessive biopsy of benign lesions raises the cost of mammographic screening[18] and results in emotional and physical burden to hundreds of thousands of patients every year, as well as financial burden to society. Thus, it would be exceedingly valuable to produce computer-aided diagnosis (CADx) systems that could aid in the decision to recommend biopsy or recommend short-term follow-up mammography. Those very likely benign cases may be managed with short-term follow-up, which will avoid a huge number of unnecessary biopsies while maintaining the very high sensitivity of cancer detection.[19,20] Moreover, since it is estimated that about half of missed cancers are missed due to misinterpretation rather than oversight,[21] it may be possible to increase the sensitivity of mammography through CADx.

### 27.1.3 BRIEF HISTORY OF CADX

CADx in breast imaging started in earnest in the early 1990s, and there have literally been hundreds of publications in the literature. Most of the major papers have been in *Medical Physics* and *Academic Radiology*, with occasional clinical evaluations in *Radiology* and *AJR*.

Many reviews of the field have been written.[22–24] Among recent efforts in particular, Giger provides a broad overview of the state of the art in CAD and CADx,[25] and Sampat et al. provide a detailed summary of the many different approaches employed and performance results attained.[26] In the following sections, citations will be provided to other representative and/or recent publications in the context of the major challenges still faced in CADx research.

## 27.2 CADX CLASSIFIER MODELS

There is no universal structure for CADx systems, but most do follow the general flowchart that is very similar to that of CAD systems (see Fig. 27.1). In this example, the system allows for inputs from three different sources: computer-extracted image-processing features, radiologist-interpreted findings, and patient history findings. The various features are selected according to some rationale, then merged together using a classifier. Each of these steps are explained in further detail in the following sections.

### 27.2.1 LINEAR VERSUS NONLINEAR CLASSIFIERS

Much of the early work in CADx was based on the artificial neural network (ANN) nonlinear classifier, which is described in many classic texts.[27–29] Neural networks were quickly embraced by the field, and this history is reviewed below to make an important cautionary note.

An example of the model architecture is shown in Fig. 27.2.